Alkylation Effects on Strong Collisions of Highly Vibrationally Excited Alkylated Pyridines with CO_2†

Qingnan Liu, Juan Du, Daniel K. Havey, Ziman Li, Elisa M. Miller,‡ and Amy S. Mullin*

Department of Chemistry and Biochemistry, University of Maryland, College Park, Maryland 20742

Received: November 21, 2006; In Final Form: February 8, 2007

The role of alkylation on the energy partitioning in strong collisions with CO_2 was investigated for highly vibrationally excited 2-ethylpyridine (2EP) and 2-propylpyridine (2PP) prepared with $E_{vib} \approx 38\,570$ and 38 870 cm^{-1}, respectively, using $\lambda = 266$ nm light. Nascent energy gain in CO_2 (00^00) rotation and translation was measured with high-resolution transient absorption spectroscopy at $\lambda \approx 4.3$ μm and the results are compared to earlier relaxation studies of pyridine ($E_{vib} = 37\,950$ cm^{-1}) and 2-methylpyridine (2MP, $E_{vib} = 38\,330$ cm^{-1}). Overall, the alkylated donors impart less rotational and translational energy to CO_2 than does pyridine. 2PP consistently imparts more translational energy in collisions than does 2EP and has larger energy transfer rates. Of the alkylated donors, 2MP and 2PP have larger probabilities for strong collisional energy transfer than does 2EP. Two competing processes are discussed: donors with longer alkyl chains have lower average energy per mode and fewer strong collisions but longer alkyl chains increase donor flexibility, leading to higher state densities that enhance energy loss via strong collisions. A comparison of state density effects based on Fermi's Golden Rule shows that 2PP has more strong collisions than predicted while 2EP has fewer. The role of torsional motion in the hot donors is considered. Comparison of effective impact parameters shows that the alkylated donors undergo strong collisions with CO_2 via a less repulsive part of the intermolecular potential than does pyridine.

Introduction

Alkane-containing hydrocarbons are primary constituents of combustion fuels, and their chemistry under high-temperature conditions is determined in part by reactivity and in part by their collisional behavior.[1] By use of master equation modeling of multicomponent multireaction processes, Miller and Klippenstein find that rate coefficients for thermal dissociation and recombination processes are not particularly sensitive to the shape of the energy transfer distribution function and that average energy transfer values suffice to describe such processes.[2,3] They point out however that this is not necessarily the case for bimolecular reactions that take place over potential energy wells, a situation in which a more accurate description of energy transfer may be required for accurate modeling. In the work presented here, we have measured the energy transfer dynamics for strong collisions of highly vibrationally excited alkylated pyridines with CO_2 using high-resolution transient IR absorption to gain a more in-depth understanding of the molecular features that impact collisional energy transfer of alkylated hydrocarbons.

The chemistry and collisional properties of alkanes are often a function of chain length.[4,5] Walker and Morley, for example, report that the product branching ratio in the reaction of alkyl radicals + O_2 at $T = 753$ K depends on the size of the alkyl reactant. The alkene + HO_2 product channel accounts for 99% for ethyl reactants, 80% for propyl reactants, and 50% for *n*-pentyl reactants.[6] Tardy and Song used time-resolved optoacoustic spectroscopy to measure energy transfer from a series of vibrationally excited fluorinated alkanes in collisions with argon.[7] For fluorinated propane through octane with $E_{vib} = 15\,000-40\,000$ cm^{-1} they measured a decrease by 30% in energy transfer rates as the number of modes in the donor is increased by a factor of 2.7. They attribute this behavior to the presence of low-frequency vibrational gateway modes that remain well populated through rapid intramolecular vibrational redistribution (IVR). Molecules with longer chain lengths have a lower average energy per mode as the number of effective vibrational modes increases for a given total energy.

The flexibility of alkylated molecules has also been recognized for enhancing collisional energy transfer. By use of time-resolved IR fluorescence (IRF), Toselli and Barker found that toluene initially excited with 248-nm light had larger average energy transfer values than benzene for a number of atomic and molecular collision partners.[8] Other groups have used UV absorption (UVA)[9] and kinetically controlled selective ionization[10] to look at toluene relaxation, but they have not performed comparable studies on benzene. A direct comparison between the UVA and IRF results is difficult due to differences in experimental calibration. From time-resolved UV absorption studies, Hippler, Troe, and Wendelken report that the collisional deactivation of substituted cycloheptatrienes ($E_{vib} = 41\,900$ cm^{-1}) with rare gases is 30−40% more efficient on average for the isopropyl donor than for the ethyl donor.[11] For molecular collision partners though, the dependence of the average energy loss on alkyl substitution is less pronounced. Linhananta and Lim showed in quasiclassical trajectory calculations of collisions of vibrationally hot ethane or propane with rare gases that methyl rotors act as gateway modes and can introduce additional pathways that enhance collisional relaxation.[12,13] They find that hindered rotors at low energy act like normal vibrations, but torsional rotors can enhance collisional energy transfer in two ways. For a free rotor, internal torsion acts like internal rotation

† Part of the special issue "James A. Miller Festschrift".

* To whom correspondence should be addressed. E-mail: mullin@umd.edu.

‡ Current address: Department of Chemistry and Biochemistry, University of Colorado, Boulder.

10.1021/jp067743c CCC: $37.00
Published on Web 03/21/2007

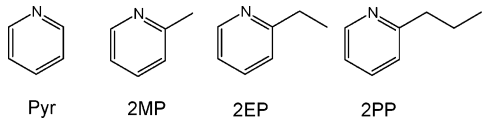

Figure 1. Vibrationally excited donor molecules compared in this study: Pyr, 2MP, 2EP, and 2PP. Excitation with $\lambda = 266$ nm light generates vibrationally excited molecules with $E_{vib} = 37\,950$, 38 330, 38 570, and 38 870 cm^{-1}, respectively.

and converts vibrational energy to external rotation in vibrationally hot molecules. This mechanism serves as a gateway for V→R, torsion energy transfer. At high energies, any hindered rotor acts like a nearly free rotor, again enhancing vibrational relaxation. Collisional relaxation of vibrationally hot propane is more effective than that of ethane because propane has more torsional degrees of freedom and a higher vibrational state density.

Not all simulations find that methyl rotors enhance collisional energy transfer. Bernshtein and Oref compared the collisional relaxation of vibrationally excited benzene, toluene, *p*-xylene, and azulene with argon and with cold benzene.[14,15] When the donor molecules are prepared with the same initial vibrational energy ($E_{vib} \approx 41\,000$ cm^{-1}), the average vibrational energy loss in collisions with cold benzene is smaller for the methylated donors than for benzene or azulene. The fact that azulene has more efficient energy transfer than *p*-xylene even though they have the same number of modes suggests that the low-frequency methyl rotors of toluene and *p*-xylene actually inhibit energy transfer by pulling energy away from the rest of the molecule. In collisions with argon, however, the authors find that energy transfer values for the alkylated donors are larger than for benzene, and they conclude that the presence of methyl rotors does not inhibit collisional energy transfer. For both the atomic and polyatomic collision partners, large energy transfer values correlate with the presence of low-frequency gateway modes in the aromatic ring.

Previously, we showed for a series of highly vibrationally excited methylated pyridines ($E_{vib} = 38\,300$ cm^{-1}) that the energy partitioning and distribution of strong collisions having $\Delta E > 3000$ cm^{-1} with CO_2 are affected by the presence of methyl groups.[16,17] The rotational and translational energy distributions of the scattered CO_2 molecules are reduced when the number of methyl groups in the vibrationally hot donor molecule is increased. The probability of strong collisions with $\Delta E > 4000$ cm^{-1} is reduced by 46% for 2-methylpyridine (2MP) relative to pyridine. The probability of collisions with ΔE values between 3000 and 4000 cm^{-1} however is increased by 17% for 2MP relative to those for pyridine. The energy transfer probability distributions for these molecules fit to single-exponential functions for $\Delta E > 3000$ cm^{-1}. Interestingly, the curvature of the exponential decay for 6 different donors correlates with the energy dependence of the vibrational state density of each donor. This group of energy donors ranges in size from pyrazine with 24 vibrational modes to 2,6-dimethylpyridine with 45 modes.

We have measured the energy partitioning of strong collisions of 2-ethylpyridine (2EP, $E_{vib} = 38\,570$ cm^{-1}) and 2-propylpyridine (2PP, $E_{vib} = 38\,870$ cm^{-1}) with CO_2 to develop a better understanding of how longer chain alkyl groups impact collisional energy transfer. Figure 1 shows the structure of these molecules along with those for pyridine and 2MP. Here we find that the probability for strong collisional energy transfer is further reduced for 2EP relative to 2MP. The propylated donor, however, exhibits more strong collisions than does 2EP. We compare the curvature of the energy transfer distribution functions to the state density energy dependence for a series of alkylated and non-alkylated donors and see deviations from linear behavior for the ethyl and propyl species. We discuss these results in terms of the competing roles of internal energy content, vibrational mode frequencies, and larger amplitude motion that results from the increased flexibility of longer alkyl chains.

Experimental Methods

State-resolved energy transfer measurements were performed using a high-resolution transient IR diode laser absorption spectrometer that has been described in detail previously.[18] A 1:1 mixture of donor and CO_2 gases was introduced to a 300 cm flowing gas collision cell with 20 mTorr total pressure at $T = 296$ K. The vibrationally excited donor molecules were prepared using 5 ns pulsed 266 nm excitation from a Nd:YAG laser, followed by rapid radiationless decay to highly vibrationally excited levels of the ground electronic state.[19,20] The UV power was kept at less than 1 MW/cm^2 to minimize multiphoton absorption. The fraction of vibrationally excited donor molecules was <15%. Energy gain in individual CO_2 rotational states was monitored by tuning a single mode diode laser operating near $\lambda = 4.3$ μm with a spectral resolution of $\Delta\nu_{IR} = 0.0003$ cm^{-1} to individual ro-vibrational transitions of CO_2 and monitoring the time-resolved fractional IR absorption following the UV pulse. The diode laser output frequency was locked to the center of the transition using a CO_2 reference cell and active feedback control. Nascent translational energy distributions were obtained by measuring transient Doppler broadened line profiles for the scattered CO_2 molecules. Line profiles were measured by locking the IR laser to a scanning Fabry Perot etalon and tuning over a CO_2 rotational line. Rotational populations and line profiles were measured at $t = 1$ μs following the UV pulse. The average collision time in the collision cell was ~4 μs. Donor molecules were degassed by several freeze−pump−thaw cycles prior to use. The following materials were used in this study: 2EP (C_7H_9N, ACROS 98+% purity), 2PP ($C_8H_{11}N$, Alfa Aesar 98% purity), and CO_2 (Matheson, 99.995% purity).

Results and Discussion

We have characterized the strong collisions of CO_2 with highly vibrationally excited 2EP and 2PP by measuring the rotational and translational energy distributions of scattered CO_2 molecules in high rotational states with $J = 62-78$. Converting lab-frame translational energy distributions into the center-of-mass frame yields the amount of donor vibrational energy that goes into translation. The rotational and translational energy gain profiles are combined with absolute energy transfer rate measurements to produce energy transfer distribution functions for strong collisions with $\Delta E > 3000$ cm^{-1}.[21] The probability distributions account for all transferred energy except the amount that goes into rotation of the donor. There is currently not a definitive way to measure the donor rotational energy after collisions. In the following sections we present the transient energy partitioning results for CO_2 energy gain and report the resulting distribution functions. Results for 2EP and 2PP collisions are compared throughout with those from earlier studies on pyridine (Pyr) and 2MP.[16]

1. Transient Absorption for CO_2 (00^00) Following Collisions with 2EP and 2PP. Collisions of CO_2 with vibrationally excited donors 2EP and 2PP result in a loss of vibrational energy from the donors and a gain in rotational and translational energy of CO_2, shown by eq 1.

$$\text{Donor}\ (E_{vib}) + CO_2 \xrightarrow{k_2^J} \text{Donor}\ (E_{vib}-E) + CO_2\ (00^00,\ J,V) \quad (1)$$

Population increases in high rotational states ($J = 62-78$) of CO_2 molecules with velocity V were monitored by high-resolution transient IR absorption at $\lambda \approx 4.3\ \mu$m. The IR probe transitions were the P-branch of the CO_2 $\nu_3 = 2349\ cm^{-1}$ antisymmetric stretching mode, shown in eq 2.

$$CO_2\ (00^00,\ J,V) + h\nu\ (\lambda \sim 4.3\ \mu m) \rightarrow CO_2\ (00^01,\ J-1,V) \quad (2)$$

Transient absorption signals for appearance of the CO_2 (00^00, $J = 62$) state following collisions with vibrationally hot 2EP and 2PP are shown in Figure 2. The signals are linear for the first few μs, where single collision conditions predominate. The fractional absorption is converted to the number density of scattered CO_2 molecules using IR transition line strengths.[22,23]

2. Product Translational Energy via Appearance of CO_2 (00^00) $J = 62-78$. The velocity distributions of scattered CO_2 molecules in high J states were determined from Doppler-broadened line profiles collected at $t = 1\ \mu$s following optical excitation of the donor molecules. Figure 3 shows a Doppler-broadened line profile for the CO_2 $J = 74$ state following collisions with 2EP and 2PP. In Figure 3, the fractional IR absorption signals (filled circles) are fit to a Gaussian function (solid line). The line profiles are broadened relative to the initial line widths at 298 K (dashed line). The full width half-maximum linewidths are reported in Table 1 along with T_{trans}(lab) and T_{trans}(com), the translational temperatures in the lab frame and the center-of-mass frame respectively.

Figure 4 compares the product center of mass translational energy for the four different pyridine donors: Pyr, 2MP, 2EP, and 2PP. The effect of alkylation is clear from the top plot: pyridine imparts more translational energy in collisions than do the alkylated donors. The product translational energy values are nearly the same for the alkylated donors. However, when data for the three alkylated donors are compared in the lower plot of Figure 4, it is seen that 2MP consistently results in more product translational energy than do 2EP or 2PP. This observation is consistent with what one would expect for impulsive collisions of different-sized donor molecules containing nearly the same internal energy. The internal energy is spread among more degrees of freedom as the number of vibrational modes increases and less energy is imparted through collisions. The addition of alkyl groups in particular introduces low frequency torsions and hindered or nearly free rotors that are preferentially populated by IVR.

This statistical trend in product translational energy is not seen when the strong collisions of 2EP and 2PP are compared. The products of strong collisions of 2PP have more translational energy than those for 2EP, even though 2PP has less energy per mode on average than 2EP. This observation suggests that longer alkyl chains can increase the translational energy of products from strong collisions due to the larger amplitude motion that comes from increased chain length. The difference in the translational energies for collision products of 2EP and 2PP is relatively small and the translational energy distributions from 2EP and 2PP are the same within experimental error as listed in Table 1. However, 2PP consistently exhibits larger energy releases than 2EP and the relative uncertainty is less than the absolute uncertainty. In section 5, the strong collisions of the alkylated donors are compared in more detail.

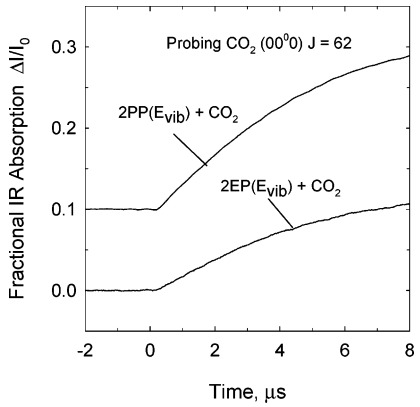

Figure 2. Transient IR absorption signals for appearance of $CO_2(00^00)$ $J = 62$ from collisions CO_2 at 300 K with vibrationally excited 2EP and 2PP (offset for clarity). Nascent CO_2 populations are determined from the IR signal at $t = 1\ \mu$s. The average time between collisions is $\sim 4\ \mu$s.

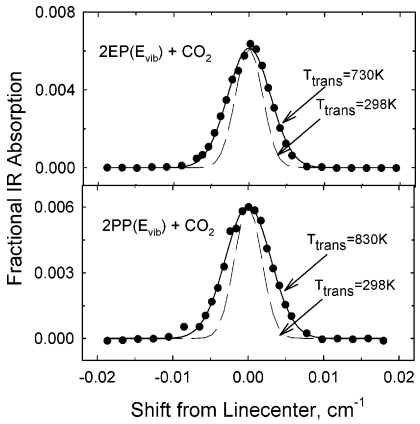

Figure 3. Nascent Doppler-broadened line profiles for $CO_2(00^00)$ $J = 74$ following collisions with vibrationally excited 2EP (a) and 2PP (b). Black circles are IR absorption at $t = 1\ \mu$s. Each line profile is fit to a Gaussian function shown as a solid line. The translational temperature T_{trans} for the scattered CO_2 molecules is determined from the full width at half-maximum line width. Transient line widths are all broadened relative to the initial 298 K profiles, shown as dashed lines. Collisions with 2PP consistently have broader line widths than 2EP indicating that the propylated donor has more vibration-to-translation energy transfer than 2EP.

3. Rotational Energy Gain in CO_2 (00^00) from 2EP and 2PP. Nascent rotational energy distributions were determined for $CO_2(00^00)$ with $J = 62-78$ that scatter from vibrationally hot 2EP and 2PP. Figure 5 shows semilog plots of the CO_2 populations measured at $t = 1\ \mu$s as a function of CO_2 rotational energy for both donors. The rotational temperature T_{rot} for scattered CO_2 molecules is determined from the slope, which equals $-k_B T_{rot}$, where k_B is Boltzmann's constant. The CO_2 rotational distributions for collisions with both donors are nearly the same: $T_{rot} = 590 \pm 60$ K for 2EP collisions and $T_{rot} = 600 \pm 60$ K for 2PP. This result is nearly identical for quenching of 2MP where $T_{rot} = 616 \pm 60$ K for the scattered CO_2. The average change in CO_2 rotational energy for the alkylated donors is $\langle \Delta E_{rot} \rangle = k_B(T_{rot} - T_0) = 210\ cm^{-1}$. In contrast, the scattered high-J CO_2 molecules have a rotational temperature of $T_{rot} = 835$ K when pyridine is the energy donor. Pyridine collisions result in a larger average increase in CO_2 rotational energy of $\langle \Delta E_{rot} \rangle = 373 \pm 60\ cm^{-1}$. Thus we find that donor alkylation reduces the amount of energy that goes into CO_2 rotation and that this effect is similar for methyl, ethyl, and propyl substituents.

TABLE 1: Doppler-Broadened Linewidths for Scattered CO_2 (00^00) for Strong Collisions of Vibrationally Excited 2EP and 2PP

	CO_2 (00^00)				
donor	J	E_{rot}, cm^{-1}	$\Delta\nu_{obs}$,[a] cm^{-1}	T_{trans}(lab),[b] K	T_{trans}(com),[c] K
2EP	62	1522.1611	0.0058[e]	560 ± 168	669 ± 201
$E_{vib} = 38\,570\ cm^{-1}$	66	1722.9413	0.0062	640 ± 192	781 ± 234
	68	1827.9724	0.0063	650 ± 195	796 ± 239
	70	1936.0953	0.0067	730 ± 219	908 ± 273
	72	2047.3081	0.0066	720 ± 216	894 ± 268
	74	2162.6090	0.0066	730 ± 219	908 ± 273
	78	2399.4677	0.0066	730 ± 219	908 ± 273
2PP	62	1522.1611	0.0063	645 ± 194	772 ± 232
$E_{vib} = 38\,870\ cm^{-1}$	66	1722.9413	0.0068	760 ± 228	928 ± 279
	68	1827.9724	0.0071	833 ± 250	1028 ± 308
	70	1936.0953	0.0071	830 ± 249	1024 ± 307
	72	2047.3081	0.0071	830 ± 249	1024 ± 307
	74	2162.6090	0.0071	843 ± 253	1042 ± 313
	76	2278.9962	0.0074	910 ± 273	1133 ± 340

[a] The full-width half-maximum line width from fitting the $t = 1\ \mu s$ transient line profile to a Gaussian function. The uncertainty in linewidths is $\pm 0.001\ cm^{-1}$. [b] The lab frame translational temperature is found using $T_{trans}(lab) = ((mc^2)/(8k_B \ln 2))((\Delta\nu_{obs})/(\nu_0))^2$ where m is the mass of CO_2, c is the speed of light, k_B is Boltzmann's constant, ν_0 is the IR transition frequency, and $\Delta\nu_{obs}$ is the nascent Doppler broadened line width. [c] The center of mass translational temperature for an isotropic distribution of scattered molecules is found using $T_{trans}(com) = T_{trans}(lab) + (T_{trans}(lab) - T_0) \times (m_{CO_2}/m_{donor})$ where $T_0 = 298$ K is the precollision temperature.

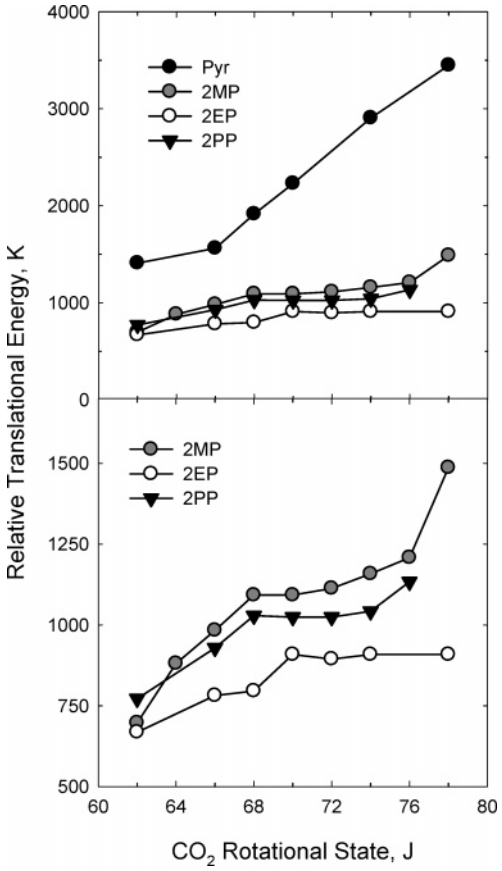

Figure 4. Relative translational temperatures T_{trans}(com) between recoiling donors and CO_2 (00^00) J = 62−78. The lower graph shows data for 2EP and 2PP along with earlier results for 2MP. The increase in T_{trans}(com) with CO_2 J state is consistent with an impulsive energy transfer mechanism. For a given J state, T_{trans}(com) generally follows the ordering of 2MP > 2PP > 2EP. The top graph compares T_{trans}(com) of the alkylated donors with those for pyridine (Pyr) and shows that alkylation substantially reduces the translational energy of the scattered molecules.

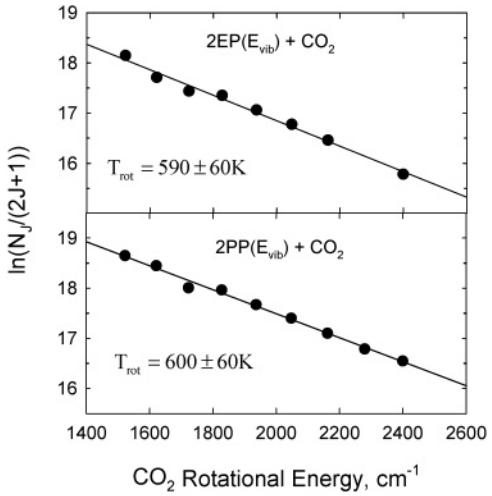

Figure 5. Nascent $t = 1\ \mu s$ rotational distributions of scattered CO_2 (00^00) with $J = 62-78$ following collisions with vibrationally hot donors 2EP and 2PP. The distribution for 2MP is similar with $T_{rot} = 610$ K. Increasing the alkyl chain length on the pyridine donor from methyl through propyl has little effect on the rotational energy of the scattered CO_2.

Changes in angular momentum ΔL that result from impulsive collisions are expected to scale as the product of the impact parameter b, reduced mass μ, and change in recoil velocity, such that $\langle\Delta L\rangle \approx b\mu\langle\Delta v_{rel}\rangle$ where ΔL is equal to the sum of rotational angular momentum changes for the colliding molecules. Figure 4 shows that, for similar J states of CO_2, the alkylated donors have smaller changes in recoil velocity than does pyridine. This result indicates that the alkylated donors undergo strong collisions at larger impact parameters than nonalkylated donors. An impact parameter for each donor with final CO_2 J state was estimated from the data in Figure 4 using the average velocity at $T = 298$ K for the initial velocity $\langle v_i\rangle = (3k_BT/\mu)^{1/2}$ and an initial CO_2 J value of $\langle J_i\rangle \approx 28$, as has been described previously.[24,25] An effective impact parameter b_{eff} for each donor:CO_2 pair was determined by averaging over the CO_2 J states for each donor and considering only the angular momentum changes for the CO_2 bath. Currently there is no direct way to measure the rotational state of the hot donor molecule. The strong collisions of pyridine with CO_2 are characterized by $b_{eff} = 1.4$ Å and the alkylated donors 2MP, 2EP, and 2PP have $b_{eff} = 2.9$, 4.0, and 3.3 Å, respectively. The ratio of b_{eff} to the Lennard-Jones σ parameter provides some information about the region of the donor:CO_2 interaction potential that is probed in our experiments. The Lennard-Jones σ parameters for the

TABLE 2: Rate Constants for Energy Gain in CO_2 (00^00, J) Following Collisions with Highly Vibrationally Excited 2EP and 2PP

CO_2 (00^00)		k_2^J, 10^{-13} cm^3 molecule^{-1} s^{-1}	
J state	E_{rot}, cm^{-1}	2EP, E_{vib} = 38 570 cm^{-1}	2PP, E_{vib} = 38 870 cm^{-1}
62	1522.1611	15.7 ± 4.7	20.0 ± 6.0
64	1621.0037	11.3 ± 3.4	17.0 ± 5.1
66	1722.9413	8.7 ± 2.6	11.1 ± 3.3
68	1827.9724	7.6 ± 2.3	11.1 ± 3.3
70	1936.0953	6.2 ± 1.9	8.5 ± 2.6
72	2047.3081	4.5 ± 1.4	6.7 ± 2.0
74	2162.6090	3.5 ± 1.1	5.1 ± 1.5
76	2278.9962	2.6 ± 0.8	3.8 ± 2.3
78	2399.4677	2.0 ± 0.6	3.1 ± 0.9
k_2^{int}, 10^{-12} cm^3 molecule^{-1} s^{-1}		6.2 ± 1.9	8.6 ± 2.6

donor:CO_2 pairs are 4.87, 5.04, 5.28, and 5.45 Å for pyridine, 2MP, 2EP, and 2PP (see Supporting Information). The ratio of $b_{eff}/\sigma = 29\%$ for pyridine, while for the alkylated 2MP, 2EP, and 2PP donors, $b_{eff}/\sigma = 57$, 75, and 60%, respectively. This result shows that the collisions studied here probe different regions of the intermolecular potential and are sensitive to donor alkylation. In each case, the collisions have b_{eff} values that are less than σ, showing that the repulsive part of the potential is involved in the relaxation, but collisions of the alkylated donors are apparently less repulsive than the pyridine collisions. This result is most likely due to the lower average energy per mode in the alkylated donors. Other factors could also contribute, including structural and electrostatic differences that are affected by high levels of vibrational excitation. For example, the similarity of b_{eff}/σ for 2MP and 2PP may suggest that the propyl group in 2PP is not fully extended during collisions with CO_2.

4. Energy Transfer Rate Constants for 2EP and 2PP with CO_2. State-resolved rate constants k_2^J for energy transfer from 2EP and 2PP to CO_2 via strong collisions were determined by measuring the early time appearance of rotational states of CO_2, as shown in eq 1. CO_2 populations were measured at $t = 1$ μs after donor excitation where the donor and CO_2 bath concentrations are essentially given by their respective values at $t = 0$. Under these early time conditions, rate constants were determined for known initial donor and CO_2 bath concentrations using eq 3.

$$k_2^J = \Delta[CO_2(00^00,J)]/[\text{Donor}(E_{vib})]_0[CO_2]\Delta t \qquad (3)$$

The scattered CO_2 populations include contributions from the Doppler-broadened line widths. The rate constants for the strong collisions that quench 2EP and 2PP are listed in Table 2.

Figure 6 compares the energy transfer rates for pyridine, 2MP, 2EP, and 2PP with CO_2. Generally, the ordering of rates goes as 2PP > 2MP > 2EP > Pyr. To account for differences in the collision rates for the different donors, it is convenient to compare the energy transfer on a per-collision basis by normalizing the energy transfer rate to the collision rate. The collision rate depends on the collisional cross section, reduced mass and translational temperature. The Lennard-Jones collision rates for the donor molecules are $k_{LJ} = 5.58 \times 10^{-10}$ for pyridine:CO_2, 5.86×10^{-10} for 2MP:CO_2, 6.39×10^{-10} for 2EP:CO_2, and 6.76×10^{-10} cm^3 molecule^{-1} s^{-1} for 2PP:CO_2. Details of the collision rate calculation are shown in Supporting Information. For these donors, the cross section has the largest effect on the collision rate. The reduced mass of 2PP−CO_2 is 14% larger than that for Pyr−CO_2, making the collision velocity for 2PP−CO_2 only ~6% smaller than that for Pyr−CO_2. The collisional cross section for 2PP−CO_2 is 30% larger than for Pyr−CO_2 and the collision rate for 2PP−CO_2 is 21% larger than for Pyr−CO_2. Energy transfer probabilities P_J were calculated by $P_J = k_2^J/k_{LJ}$ and are shown in Figure 6 for the four donor−CO_2 pairs. Compared on a per-collision basis, the ordering of energy transfer probability goes as 2PP ≈ 2MP > 2EP > Pyr with the J-specific probabilities for 2PP relaxation being about twice those of pyridine. The observed ordering of energy transfer probabilities may be a result of increasing state density in the larger donor molecules. Comparison with the other donors shows that 2MP has larger rates and probabilities than 2EP, which is not predicted on the basis of donor size.

5. $P(\Delta E)$ Curves for Strong Collisions with CO_2. Energy transfer distribution functions for strong collisions of 2EP and 2PP with CO_2 were determined from measurements of rate constants and CO_2 energy gain by considering the combined distribution of rotational and translational energy for the scattered CO_2 molecules. The procedure for this transformation has been presented previously and the essential points are discussed here.[21] The key idea is to convert from state- and velocity-indexed data to a ΔE-indexed probability. Each J state of CO_2 has a velocity distribution whose width is specified by the spectral Doppler-broadening and a probability that is determined by the ratio of the rate constant to the collision rate. The probability distribution for the change in energy ΔE is obtained by subtracting the average initial rotational and translational energies. The overall energy transfer probability distribution function $P(\Delta E)$ results from summing over the distribution functions of individual CO_2 J states. The only assumptions in this transformation are the values of the precollision energies and the collision rate. Scattered CO_2 molecules in low J states have not been characterized in these studies so the $P(\Delta E)$ curves are complete for $\Delta E > 3000$ cm^{-1}. Contributions to ΔE from donor rotation are not accounted for in the probability distributions. Simulations indicate that donor molecules can gain rotational energy through quenching collisions, but this effect is most pronounced in collisions with rare gas atoms.[26] The extent of rotational energy gain in the donors is expected to be less than for CO_2 based on the conservation of angular momentum and the relatively small rotational constants for the donor molecules.

The energy transfer distribution functions for the strong collisions of Pyr, 2MP, 2EP, and 2PP with CO_2 are shown in Figure 7. The distributions in Figure 7 are normalized to the Lennard-Jones collision rates. Pyridine has the largest probability for strong collisions with $\Delta E > 4000$ cm^{-1}. Among the alkylated donors, 2MP and 2PP have similar $P(\Delta E)$ curves while 2EP has the lowest probability for strong collisions. Figure 7 highlights several important features for strong collisions with CO_2. Strong collisional energy transfer is favored for smaller donor molecules that on average have more energy per mode than do the larger donor molecules. The alkylated donors have less energy per mode on average than do non-alkylated donors and in general the likelihood of strong collisions for these former donors is reduced. The probability of relaxation via strong collisions with $\Delta E > 4000$ cm^{-1} has the order Pyr > 2MP > 2EP. However, this trend does not continue for 2PP. For the alkylated donors, the probability of strong collisions is ordered as 2MP ≈ 2PP > 2EP.

2PP imparts substantially more energy to the rotational and translational degrees of freedom of CO_2 in single collision transitions with $\Delta E > 3000$ cm^{-1} than does 2EP. This result is not consistent with the lower average energy per mode of 2PP. It is possible that differences in the potentials of the torsional and methyl rotor vibrations of the various donors contribute to

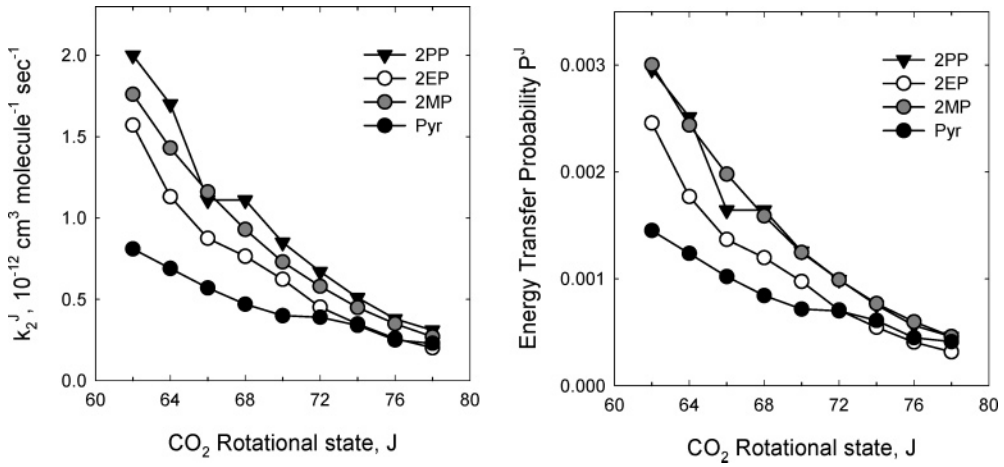

Figure 6. Absolute rate constants k_2^J and energy transfer probabilities P^J for initial appearance of scattered CO_2 (00^00) $J = 62-78$ following collisions with vibrationally excited donors. The ordering of energy transfer rates for appearance of a given CO_2 J state is 2PP > 2MP > 2EP. The rates for energy transfer from the alkylated donors are larger than those from Pyr.

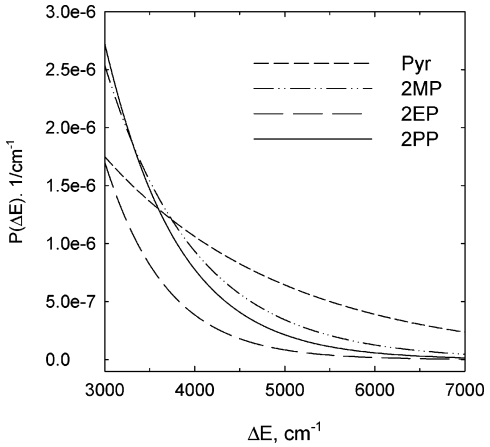

Figure 7. Comparison of $P(\Delta E)$ curves for strong collisions with $\Delta E > 3000$ cm^{-1} of CO_2 with vibrationally hot donors 2EP and 2PP. 2PP has a larger probability for strong collisions than 2EP.

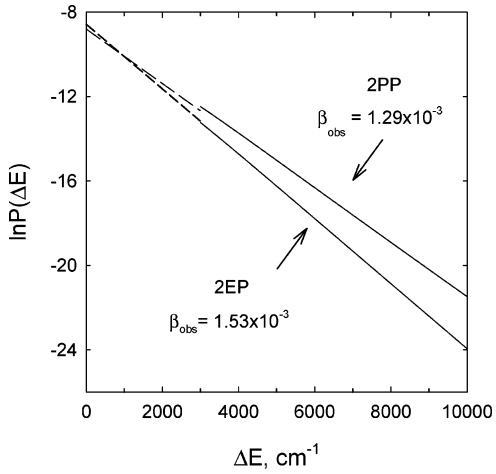

Figure 8. Semilog plot of $P(\Delta E)$ with $\Delta E > 3000$ cm^{-1} for strong collisions of vibrationally hot 2EP and 2PP with CO_2. The slope equals $-\beta_{obs}$ ΔE.

the observed differences in their $P(\Delta E)$ curves. Simulations on smaller molecules such as ethane and propane have already provided important clues as to how methyl and ethyl torsional motion can enhance vibrational relaxation, and future theoretical studies on mixed alkyl aromatic molecules may provide additional insight.[12,13] It is also possible that longer alkyl chain in 2PP introduces new dynamical effects that are not present in aromatic and methylated aromatic species. Longer-chain alkyl groups can undergo larger-amplitude motion, and whiplike motions of the propyl chain may account for the enhanced strong collisions in 2PP. The possibility for such interactions would be enhanced by chattering collisions in which the donor and bath molecules undergo multiple impulsive encounters during a single "collision." Trajectory calculations of the strong collisions between pyrazine ($E_{vib} = 38\,000$ cm^{-1}) with CO_2 find that nearly 50% of strong collisions have multiple direct encounters.[27] The simulations show that typical chattering collisions involve low relative translational energies and correspondingly small increases in internal rotation of the collision pair. Linhananta and Lim also observe chattering collisions for propane ($E_{vib} = 41\,000$ cm^{-1}) with argon and find that collisional energy transfer increases with the number of encounters.[28] The presence of this type of long-lived collision complex could help facilitate energy transfer that involves large amplitude motion of the propyl chain. It is also possible that the longer chain length of 2PP introduces new possibilities for constrained configurations that increase the mode frequencies of the propyl group. Models based on simple geometric considerations indicate that the propyl group in 2PP is long enough to form a secondary ringlike structure adjacent to the pyridine ring. Constraining the propyl group configuration would actually increase the energy content of the aromatic ring, which in turn could enhance the strong collisions. This scenario is in agreement with the simulation results of Bernshtein and Oref showing that collisional energy transfer from azulene (E_{vib}) to benzene is enhanced relative to that for *p*-xylene (E_{vib}).[14] Even though the two donors have the same number of modes, the stiffer ring system has higher frequency modes and more vibrational energy transfer. It is not clear however why the simulations do not show a similar effect when argon is the quencher.

6. Comparison of State Density and Strong Collisions for 2PP and 2EP. Earlier studies in our laboratories have shown that the curvature of the probability distribution function for strong collisions of highly excited azabenzenes and methylated azabenzenes correlates with the energy dependence of the vibrational state density. This correlation is seen for collisions with CO_2 and with H_2O.[16,17,29] Here, we explore the relationship between state density and energy transfer for the alkyated pyridines.

$P(\Delta E)$ curves such as those shown in Figure 8 characterize the probability that a vibrationally hot molecule will lose an

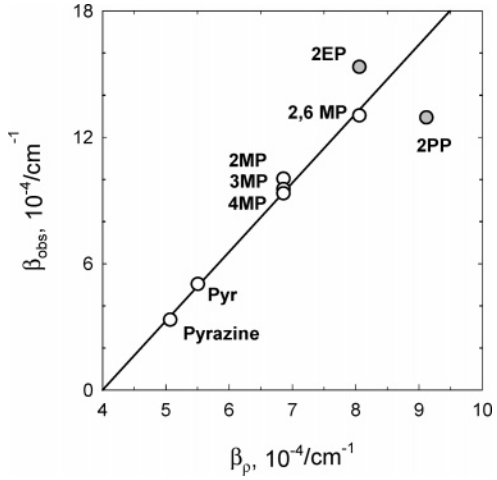

Figure 9. Comparison of β_{obs} for strong collisions and the vibrational state density energy dependence parameter β_ρ for collisions of CO_2 with highly vibrationally excited donors: pyrazine, Pyr, methylpyridine isomers (2MP, 3MP, 4MP), 2,6MP, 2EP, and 2PP. A linear correlation is seen for the unsubstituted donors and for donors containing methyl or ethyl groups. For donors with larger alkyl groups, β_{obs} no longer correlates with changes in state density associated with ΔE. In the limiting case of no rotational or translational energy gain in CO_2, β_{obs} has a value near 4×10^{-3}/cm^{-1}.

amount of energy ΔE through collisions with CO_2. The curve for each donor is fit to a single-exponential decay using eq 4

$$P(\Delta E) = \alpha_{obs} \exp(-\beta_{obs}\Delta E) \quad (4)$$

where α_{obs} and β_{obs} are fitting parameters. β_{obs} describes the relative weighting of weak to strong collisions for a given donor. The vibrational state density of the excited donors is also a function of ΔE. The state density of the donors considered here is well described by eq 5 for $\Delta E = 0$ to 10 000 cm^{-1}.

$$\rho(E - \Delta E) = \alpha_\rho \exp(-\beta_\rho \Delta E) \quad (5)$$

The parameter β_ρ characterizes how the vibrational state density changes with internal energy. Figure 9 shows the correlation between β_{obs} from the experimental probabilities and β_ρ for calculated state densities for a number of other donor molecules: pyrazine, pyridine, methylpyridine isomers (2MP, 3MP, and 4MP), and 2,6-dimethylpyridine (2,6MP). The linear fit of the data shows that the larger donor molecules have larger values of both β_{obs} and β_ρ. The $P(\Delta E)$ curves and the corresponding β_{obs} values show that donor molecules undergo energy loss transitions more readily for weaker collisions. The state density energy dependence (β_ρ) increases with the number of vibrational modes. For a given energy loss transition of ΔE, larger donor molecules have greater mismatches in their state densities before and after the collision. This mismatch correlates with a reduction in the likelihood of energy transfer relative to smaller ΔE values and leads to a steeper slope in ln $P(\Delta E)$ for the larger donor molecules, hence a larger β_ρ value. This behavior is evident from data for the non-alkylated and methylated donors in Figure 9. It is important to clarify that the data in Figure 9 provide information on the *curvature* of the energy transfer distribution functions not on the absolute probability itself. At a given internal energy, larger donor molecules have high state densities and are predicted by Fermi's Golden Rule to have larger energy transfer probabilities. Our data are generally in agreement with this prediction, but more specific correlation of the energy transfer probability with the donor state density cannot be made without additional knowledge of the matrix elements that couple the initial and final states.

The state densities for 2EP and 2PP were determined as a function of $E - \Delta E$ using donor vibrational frequencies and performing a direct count of states with the Beyer−Swinehart algorithm.[30] The vibrational modes of 2EP with frequencies above 200 cm^{-1} were measured by Green and Barnard.[31] However, the low-frequency modes that correspond to torsional motions of the ethyl group were not reported. The normal modes of 2EP and 2PP were estimated using Hartree−Fock calculations at the 6-311G** level. At this level of theory, the calculated frequencies for normal modes do not exactly reproduce the experimental results and were adjusted using established scaling factors.[32] We found however that the state density parameter β_ρ was not particularly sensitive to the exact mode frequencies and that the nonscaled frequencies yielded reliable β_ρ values. To verify this, β_ρ values were determined for pyridine, 2MP, and 2,6MP using calculated frequencies and using experimental frequencies. The resulting β_ρ values were the same within 0.7%. The state density is very sensitive to the choice of the low-frequency modes, but the β_ρ value is much less sensitive because β_ρ describes the energy dependence of the state density not the actual state density. For example, the state density of 2EP (E_{vib} = 38 570 cm^{-1}) is 10 times larger if one low-frequency mode is decreased from 200 to 20 cm^{-1}, but β_ρ is insensitive to this change, varying by less than 0.2%.

We also considered how the alkyl rotors impacted the state density calculations. Vibrational modes that correspond to internal rotations are treated differently depending on whether they are hindered or free rotors. The total energy content in the molecules is below the dissociation limit but is well above barriers to internal rotation. A one-dimensional hindered rotor potential energy $U(\varphi)$ is given in eq 6

$$U(\varphi) = \frac{V}{2}(1 - \cos(n\varphi)) \quad (6)$$

where φ is the rotation angle, n is the number of minima, and V is the barrier height. For a hindered rotor, the mode energy is less than the barrier height, $E_{mode} < V$. A free-rotor model is more appropriate at higher energies when $E_{mode} > V$. The hindered rotor model was used by Draeger[33] for the methyl group in toluene at 300 K with a barrier height of V = 720 cm^{-1}, zero-point energy E_0 = 86 cm^{-1}, and first excited state E_1 = 258 cm^{-1}. Highly vibrationally excited 2EP (E_{vib} = 38 570 cm^{-1}) has ∼1300 cm^{-1} on average in the lowest frequency mode. The average energy in this mode is far greater than the barrier height of 720 cm^{-1} for a methyl-hindered rotor in toluene, and thus it is reasonable that the methyl rotor in vibrationally excited 2EP is a free rotor. We treated the internal rotors in 2EP and 2PP as harmonic oscillators in one extreme and as free rotors the other extreme to establish limiting values of β_ρ. The state density in the free-rotor limit was determined using a modified Beyer−Swinehart method.[34] The choice of the hindered- or free-rotor model has a negligible effect on β_ρ and values for the two extremes have differences that are less than 0.1%.

The state densities for 2EP and 2PP are characterized by $\beta_\rho = 8.07 \times 10^{-4}$/cm^{-1} for 2EP and $\beta_\rho = 9.13 \times 10^{-4}$/cm^{-1} for 2PP. The parameters for energy transfer are $\beta_{obs} = 15.3 \times 10^{-4}$/cm^{-1} for 2EP and $\beta_{obs} = 12.9 \times 10^{-4}$/cm^{-1} for 2PP. These data are plotted in Figure 9 and show deviations from the linear correlation seen for the non-alkyated and methylated donors. Collisions with $\Delta E > 3000$ cm^{-1} for 2EP are not as strong as

predicted by the state density energy dependence and for 2PP the collisions are stronger than predicted. It is possible that the curvature of the probability distribution (β_{obs}) correlates with state density energy dependence (β_ρ) only holds for aromatic systems with hydrogen or methyl substituents. It is also possible that dynamical effects such as large amplitude motion of longer chain alkyl groups and ring closing mechanisms are responsible for the observed deviations. Such effects are not accounted for by statistical models. The effect of anharmonicity was not included in our state density calculations but it is unlikely that anharmonicity would lead to the observed shifts in the β_{obs} values for 2EP and 2PP.

Conclusion

We have investigated the effect of alkylation on the strong collisional energy transfer between CO_2 and a series of highly vibrationally excited alkylpyridines ($E_{vib} \sim 38\,400\ cm^{-1}$) where alkyl = methyl, ethyl, and propyl. The nascent rotational and translational energy distributions for scattered CO_2 molecules were measured under single collision conditions using high-resolution transient IR absorption. Strong collisions between pyridine and CO_2 lead to substantially more rotational and translational energy in the scattered molecules than for the alkylated donors. Differences are also seen in the distribution functions for the strong collisions of the alkylated donors. The ordering of strong collision probabilities with CO_2 is pyridine $>$ 2MP $\approx$ 2PP $>$ 2EP. The probability for strong collisions with CO_2 is twice as large for 2PP as for 2EP. Our results show that longer-chain alkyl groups actually enhance strong collisional energy transfer. This observation cannot be explained solely by describing the vibrationally hot donor molecule statistically. Possible dynamical reasons for the observed enhancement of strong collisions include large-amplitude, whiplike motion of the longer chain alkyl group and constrained geometries that put more energy into the aromatic ring.

Acknowledgment. We gratefully acknowledge research support from the Department of Energy Basic Energy Science Program (DE-FG-02-06ER15761) and equipment support from the National Science Foundation (CHE-0552663).

Supporting Information Available: Determination of collision rate constants for Pyr and 2MP, σ vs ϵ/k_B graph, table of LJ data. This material is available free of charge via the Internet at http://pubs.acs.org.

References and Notes

(1) Miller, J. A.; Pilling, M. J.; Troe, J. *Proc. Combust. Inst.* **2005**, *30*, 43.
(2) Miller, J. A.; Klippenstein, S. J. *J. Phys. Chem. A* **2006**, *110*, 10528.
(3) Fernandez-Ramos, A.; Miller, J. A.; Klippenstein, S. J.; Truhlar, D. G. *Chem. Rev.* **2006**, *106*, 4518.
(4) DeSain, J. D.; Taatjes, C. A.; Miller, J. A.; Klippenstein, S. J.; Hahn, D. K. *Faraday Discuss.* **2001**, *119*, 101.
(5) DeSain, J. D.; Klippenstein, S. J.; Miller, J. A.; Taatjes, C. A. *J. Phys. Chem. A* **2003**, *107*, 4415.
(6) Walker, R. W.; Morley, C. In *Low Temperature Combustion and Autoignition*; Pilling, M. J., Ed.; Elsevier: Amsterdam, 1997; p 1.
(7) Tardy, D. C.; Song, B. H. *J. Phys. Chem.* **1993**, *97*, 5628.
(8) Toselli, B. M.; Barker, J. R. *J. Chem. Phys.* **1992**, *97*, 1809.
(9) Hippler, H.; Troe, J.; Wendelken, H. J. *J. Chem. Phys.* **1983**, *78*, 6709.
(10) Lenzer, T.; Luther, K.; Reihs, K.; Symonds, A. C. *J. Chem. Phys.* **2000**, *112*, 4090.
(11) Hippler, H.; Troe, J.; Wendelken, H. J. *J. Chem. Phys.* **1983**, *78*, 6718.
(12) Linhananta, A.; Lim, K. F. *Phys. Chem. Chem. Phys.* **1999**, *1*, 3467.
(13) Linhananta, A.; Lim, K. F. *Phys. Chem. Chem. Phys.* **2000**, *2*, 1385.
(14) Bernshtein, V.; Oref, I. *J. Phys. Chem. A* **2006**, *110*, 1541.
(15) Bernshtein, V.; Oref, I. *J. Phys. Chem. A* **2006**, *110*, 8477.
(16) Park, J.; Shum, L.; Lemoff, A. S.; Werner, K.; Mullin, A. S. *J. Chem. Phys.* **2002**, *117*, 5221.
(17) Miller, E. M.; Murat, L.; Bennette, N.; Hayes, M.; Mullin, A. S. *J. Phys. Chem. A* **2006**, *110*, 3266.
(18) Wall, M. C.; Lemoff, A. S.; Mullin, A. S. *J. Phys. Chem. A* **1998**, *102*, 9101.
(19) Yamazaki, I.; Murao, T.; Yoshihara, K.; Fujita, M.; Sushida, K.; Baba, H. *Chem. Phys. Lett.* **1982**, *92*, 421.
(20) Sushida, K.; Fujita, M.; Yamazaki, I.; Baba, H. *Bull. Chem. Soc. Jpn.* **1983**, *56*, 2228.
(21) Michaels, C. A.; Flynn, G. W. *J. Chem. Phys.* **1997**, *106*, 3558.
(22) Roney, P. L.; Findlay, F. D.; Buijs, H. L.; Cann, M. W. P.; Nicholls, R. W. *App. Opt.* **1978**, *17*, 2599.
(23) Rothman, L. S. et al. *J. Quant. Spec. Rad. Trans.* **2005**, *96*, 139.
(24) Li, Z.; Korobkova, E.; Werner, K.; Shum, L.; Mullin, A. S. *J. Chem. Phys.* **2005**, *123*, 174306/1.
(25) Mullin, A. S.; Michaels, C. A.; Flynn, G. W. *J. Chem. Phys.* **1995**, *102*, 6032.
(26) Lenzer, T.; Luther, K. *J. Chem. Phys.* **1996**, *104*, 3391.
(27) Li, Z.; Sansom, R.; Bonella, S.; Coker, D. F.; Mullin, A. S. *J. Phys. Chem. A* **2005**, *109*, 7657.
(28) Linhananta, A.; Lim, K. F. *Phys. Chem. Chem. Phys.* **2002**, *4*, 577.
(29) Elioff, M. S.; Fang, M.; Mullin, A. S. *J. Chem. Phys.* **2001**, *115*, 6990.
(30) Stein, S. E.; Rabinovitch, B. S. *J. Chem. Phys.* **1973**, *58*, 2438.
(31) Green, J. H. S.; Barnard, P. W. B. *J. Chem. Soc.* **1963**, 640.
(32) Scott, A. P.; Radom, L. *J. Phys. Chem.* **1996**, *100*, 16502.
(33) Draeger, J. A. *Spetrochim. Acta A* **1985**, *41A*, 607.
(34) Baer, T.; Hase, W. L. *Unimolecular Reaction Dynamics: Theory and Experiments*; Oxford University Press: New York, 1996.